

**Normal-state gap in the parent cuprate  $\text{Pr}_2\text{CuO}_{4\pm\delta}$** Ge He,<sup>1,2</sup> Xinjian Wei,<sup>1,2</sup> Xu Zhang,<sup>1,2</sup> Lei Shan,<sup>1,2,3</sup> Jie Yuan,<sup>1</sup> Beiyi Zhu,<sup>1</sup> Yuan Lin,<sup>4</sup> and Kui Jin<sup>1,2,3,\*</sup><sup>1</sup>*Condensed Matter Physics, Institute of Physics, Chinese Academy of Sciences, Beijing 100190, China*<sup>2</sup>*School of Physical Sciences, University of Chinese Academy of Sciences, Beijing 100049, China*<sup>3</sup>*Collaborative Innovation Center of Quantum Matter, Beijing 100190, China*<sup>4</sup>*State Key Laboratory of Electronic Thin Films and Integrated Devices & Center for Information in Medicine, University of Electronic Science and Technology of China, Chengdu 610054, China*

(Received 10 March 2017; revised manuscript received 11 August 2017; published 28 September 2017)

We present a tunneling study on single-crystalline parent-cuprate thin films, i.e., a series of  $\text{Pr}_2\text{CuO}_{4\pm\delta}$  with tunable superconducting transition temperature. The zero-bias anomaly in the differential conductance, well-reported in the normal state of  $\text{R}_{2-x}\text{Ce}_x\text{CuO}_4$  ( $\text{R} = \text{Pr, Nd, La}$ ) and named as normal-state gap (NSG), is observed in the Ce-free samples. This NSG behaves quite robustly against magnetic fields up to 16 T, but fades away with increasing temperature. Most importantly, we find that the magnitude of the NSG becomes larger with increasing point-contact junction resistance on the superconducting films, which is further enhanced in the nonsuperconducting samples with more oxygen disorder. The origination of NSG can be understood in the framework of the Altshuler-Aronov-Lee theory, where the disorder-induced electron-electron interactions suppress the density of states and thereby result in a soft Coulomb gap.

DOI: [10.1103/PhysRevB.96.104518](https://doi.org/10.1103/PhysRevB.96.104518)

Besides the superconductivity, cuprates exhibit a great deal of anomalies, such as non-Fermi liquid behavior, pseudogap, etc., which are crucial to understanding the high  $T_c$  mechanism [1–5]. The origination of the pseudogap is a protracted struggle for hole-doped cuprates, i.e., whether it is from phase incoherent Cooper pairs or other competing orders [6–10]. In electron-doped cuprates, there are two discriminable energy scales in the normal state, that is, the higher one (0.2 ~ 0.4 eV), mimicking a pseudogap, and the so-called normal-state gap (NSG) of lower energy (NSG ~ 5 meV) [1]. The former is observed by techniques such as optical conductivity spectra [11] and angle-resolved photoemission spectroscopy (ARPES) [12], and identified as antiferromagnetic (AFM) spin correlations [13]. Nevertheless, the origin of the NSG, whose signature is a zero-bias anomaly (ZBA) in differential conductance spectra, remains controversial [14–17].

The zero-bias anomaly in tunneling spectra may stem from various reasons, such as electron-electron interactions [18], Coulomb blockade [19], hopping dominated conductance between the clusters of disordered metal grains [20], Kondo scattering from magnetic moments, Giaever-Zeller two-step tunneling process, etc. In electron-doped cuprates, Alff *et al.* studied the tunneling spectra of  $\text{Pr}_{2-x}\text{Ce}_x\text{CuO}_4$  and  $\text{La}_{2-x}\text{Ce}_x\text{CuO}_4$ , and reported a buildup temperature of NSG  $T^*$  that is smaller than  $T_c$ , pointing to a competing order below the superconducting dome [15]. However, Dagan *et al.* reported that in  $\text{Pr}_{2-x}\text{Ce}_x\text{CuO}_4$ ,  $T^*$  is slightly higher than  $T_c$  in the underdoped region and approaches  $T_c$  in the overdoped region, linked to the superconducting amplitude fluctuations [16]. By integrating the spectral weight and comparing the difference between the NSG and the superconducting state, Shan *et al.* provided evidence of a two-gap scenario in  $\text{Pr}_{1-x}\text{La}_x\text{Ce}_x\text{CuO}_4$  [17]. Such contradictions can be ascribed to the difficulty in defining  $T^*$ , as well as the side effects from oxygen. Indeed, it is known that

slight oxygen variation is inevitable when tuning the Ce, which can result in remarkable influence on the physical properties [1]. As a special system of electron-doped cuprates, the superconductivity of parent cuprates (i.e.  $\text{R}_2\text{CuO}_{4\pm\delta}$ ) in  $T'$  phase was discovered recently [21]. Most recently, optical conductivity measurements in  $\text{Pr}_2\text{CuO}_{4\pm\delta}$  (PCO) thin films disclosed that the high energy “pseudogap” does not exist in this system [22]. However, the low-energy NSG has never been addressed in this system, e.g., whether it is similar to other electron-doped cuprates or not in such a Ce-free system.

In this paper, we present a systematic tunneling study of PCO thin films with various  $T_c$  by point-contact technique. The NSG is observed in this system, which is quite similar to other electron-doped cuprates. The NSG is nearly field-independent but can be suppressed gradually by increasing the temperature. We find that there is a positive correlation between the magnitude of the NSG and junction resistance for all the superconducting samples, and the magnitude of the NSG is further enhanced in nonsuperconducting ones with more oxygen disorder. These phenomena can be well explained by the Altshuler-Aronov-Lee (AAL) theory, revealing that the NSG stems from the disorder-induced electron-electron interactions.

The PCO thin films are grown by polymer-assisted deposition [23,24] on a (001)-oriented  $\text{SrTiO}_3$  substrate [25]. The as-grown samples are fired at 850 °C in a sealed tube with oxygen pressure at 200 Pa for crystallization. Then these samples are annealed at 400–600 °C under oxygen pressure of 15 Pa. By adjusting the annealing temperature and time, samples with various  $T_c$  can be obtained. The ab-plane resistivity is measured from 2 K to 300 K by a standard four-probe method using Quantum Design PPMS-16 equipment. We have selected several samples with full transition temperature  $T_{c0} = 0$  (N1, N2), 15.5 K (S15), 16.4 K (S16), 17.8 K (S17), 19.3 K (S19), and 23.6 K (S23). Except for the nonsuperconducting samples, the others show narrow transition widths of  $\Delta T = 1 \sim 2$  K in the following measurements [26].

\*kuijin@iphy.ac.cn

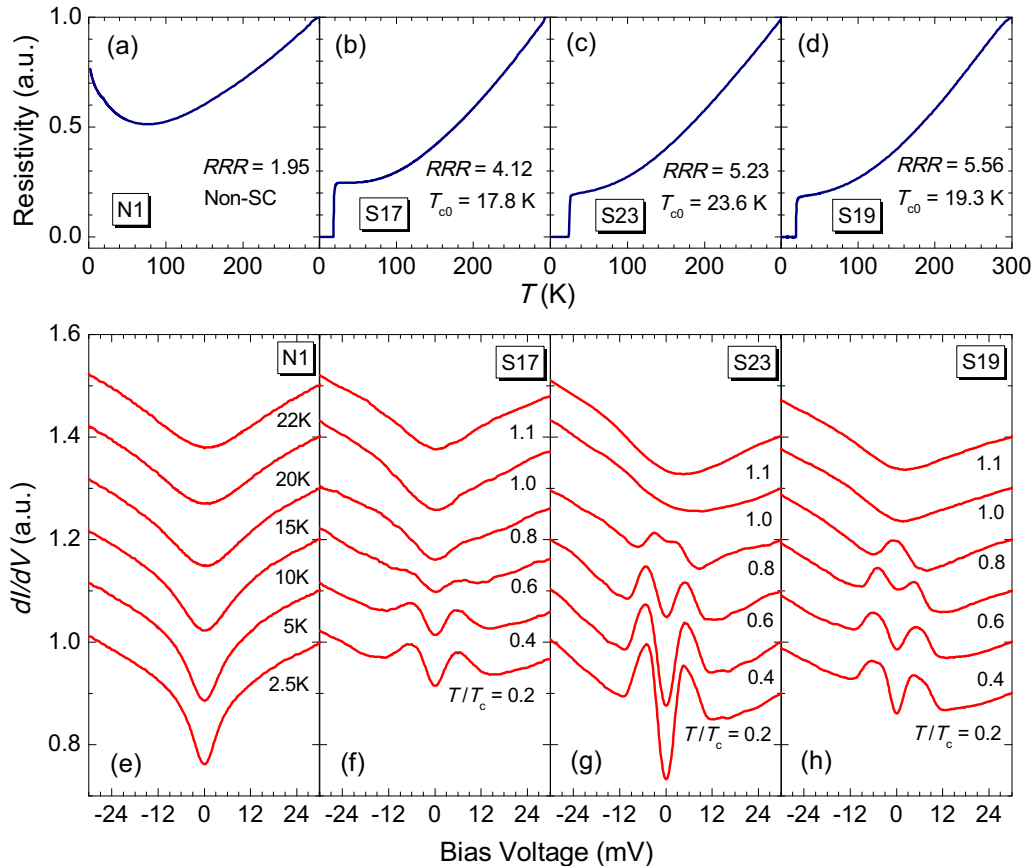


FIG. 1. (a)–(d) Temperature dependence of resistivity for parent cuprate  $\text{Pr}_2\text{CuO}_{4\pm\delta}$  thin films with various  $T_c$  and  $RRR$ . Resistivities are normalized by dividing the value at 300 K. (e)–(h)  $dI/dV$  versus bias voltage at various temperatures for these samples. All the curves are offset upwards for the sake of clarity.

Tunneling spectra measurements are performed with a homemade point-contact probe, which can be put into the PPMS to ensure the temperatures down to 2 K and fields up to 16 T. Pt/Ir tips are used to make steady point-contact junctions. We measure the differential conductance spectra with a traditional lock-in technique. The spectra have good reproducibility for the same sample in various locations on the surface. The field is perpendicular to the  $ab$ -plane of the samples in all the measurements [27].

Figures 1(a)–1(d) show the temperature dependence of the resistivity for N1, S17, S23, and S19. The residual resistance ratio (RRR) is smaller in the nonsuperconducting sample than in the superconducting ones. Since the RRR is sensitive to the amount of impurities and crystallographic defects, there should exist more disorder in the nonsuperconducting sample. In electron-doped cuprates, these defects mainly come from the apical oxygen and in-plane oxygen vacancies induced by under- or overannealing process [28,29]. Figures 1(e)–1(h) present the  $dI/dV$  versus the bias voltage at various temperatures for the corresponding samples of Figs. 1(a)–1(d). The zero-bias anomaly observed in N1 demonstrates that the NSG state exists in the nonsuperconducting samples in the absence of field [see Fig. 1(e)], as observed in nonsuperconducting  $\text{Pr}_{1.89}\text{Ce}_{0.11}\text{CuO}_4$  samples [16]. Superconducting coherence peaks are observed in all the superconducting samples, which are suppressed with increasing temperature and disappear

at  $T_c$ . The zero-bias conductance is different among these samples due to the various effective barrier heights [30].

Figure 2(a) displays the spectra for S17 in both the superconducting state and the normal state. The spectra coincide with each other at bias higher than 10 mV, whereas the NSG state appears near the zero bias when field is applied to suppress superconductivity [see Fig. 2(a)]. The spectra are almost unchanged with increasing field at  $T = 2.5$  K in N1, as seen in Fig. 2(b). As in the nonsuperconducting sample, the spectra are nearly unchanged by fields up to 16 T after suppression of the coherence peaks at  $H \sim 6$  T in S23 [see Fig. 2(c)], which is consistent with the  $H_{c2}$  measured in Ref. [31]. We define  $G(30\text{mV})/G(0)$  as the magnitude of the NSG state and plot it as a function of  $H$ , as shown in Fig. 2(d). It can be clearly seen that the NSG is hard to suppress with magnetic fields for all the samples even at  $T = 15$  K and  $H = 16$  T.

As shown in Fig. 3(a), for fields higher than  $H_{c2}$ , the zero-bias dip in the spectra is continuously filled as temperature increases. Also,  $G(30\text{mV})/G(0)$  decreases gradually with increasing temperature [see Fig. 3(b)], which is quite similar to the behaviors observed in other electron-doped cuprates [14,16,17]. Taking into account the temperature-induced Fermi function broadening effects, we calculate temperature dependence of the density of state based on the formula  $N(eV, T) = \int N(E, 0) \frac{\partial f(E - eV, T)}{\partial E} dE$ . The calculated

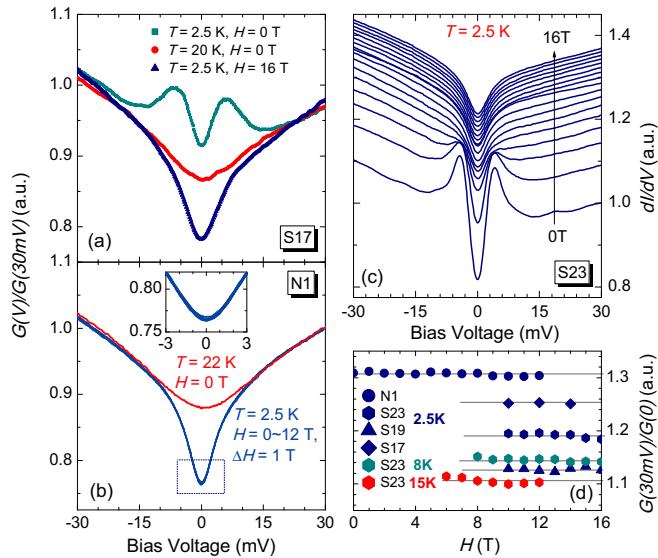


FIG. 2. (a)  $dI/dV$  versus bias voltage for S17 measured in the superconducting state (solid squares), temperature higher than  $T_c$  (solid circles) with  $H = 0$  and magnetic field higher than  $H_{c2}$  at  $T = 2.5$  K (solid triangles). (b)  $dI/dV$  of the nonsuperconducting sample at  $T = 2.5$  K,  $H = 0 \sim 12$  T with  $\Delta H = 1$  T and  $T = 22$  K,  $H = 0$  T. Inset: zoom in the spectra near the zero bias (dashed square region). (c)  $dI/dV$  versus bias voltage in different fields for S23. All curves are offset upwards for clarity. (d) Field dependence of  $G(30mV)/G(0)$  for different samples. The horizontal gray lines are guides for the eye. For superconducting samples, the data is only plotted for fields higher than  $H_{c2}$ .

$G(30mV)/G(0)$  is obviously higher than in experiments [see Fig. 3(b)], which suggests that Fermi broadening is not the main reason behind the NSG closing.

To get further insight into the NSG state, we measure the  $dI/dV$  spectra at various junction resistances ( $R_j$ ) [see Fig. 4(a)]. We find that the zero-bias dip becomes deeper and deeper as  $R_j$  increases. The magnitude of NSG versus  $R_j$  is plotted in Fig. 4(b), which shows a nearly positive relationship with  $R_j$  for all the superconducting samples. Moreover, the magnitude of NSG in N1 and N2 samples is further enhanced

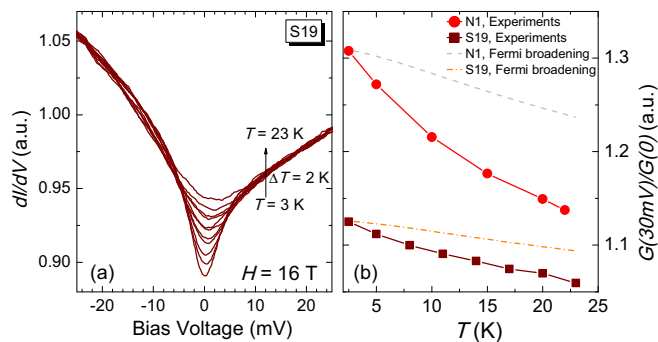


FIG. 3. (a)  $dI/dV$  for S19 at different temperatures for  $H = 16$  T. (b) Temperature dependence of  $G(30mV)/G(0)$  for S19 (solid squares) at  $H = 16$  T and N1 at  $H = 0$  T (solid circles). The calculated  $G(30mV)/G(0)$  considering Fermi broadening effects for S19 (dash dotted line) and N1 (dashed line) are plotted as a function of temperature.

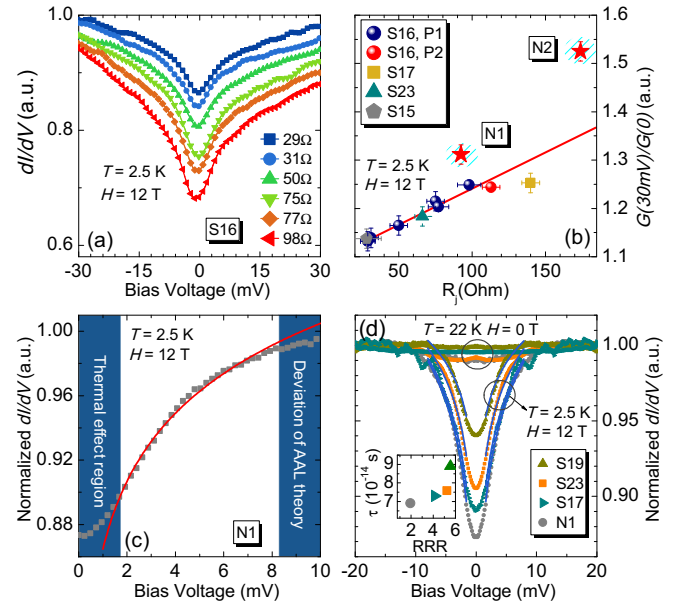


FIG. 4. (a)  $dI/dV$  versus bias voltage of S16 in different junction resistances at  $T = 2.5$  K and  $H = 12$  T. (b)  $G(30mV)/G(0)$  versus junction resistance for different samples. The data of the superconducting samples can be fitted with a solid line. The  $G(30mV)/G(0)$  values of the nonsuperconducting samples (star) are higher than that of the superconducting samples at the same junction resistance. (c) Normalized  $dI/dV$  versus bias voltage for N1 at  $T = 2.5$  K,  $H = 12$  T (solid squares). The data is fitted with the AAL theory (solid lines). (d) Normalized  $dI/dV$  versus bias voltage for different samples at  $T = 2.5$  K,  $H = 12$  T and  $T = 22$  K,  $H = 0$  T. All the data can be well fitted in the range of  $2 \sim 8$  mV (solid lines). Inset: RRR dependence of the relaxation time  $\tau$ .

compared to the superconducting samples. The increased  $R_j$  is due to a variation of the point-contact size. In addition,  $R_j$  also has a positive correlation with the thickness of the effective barrier [30]. In the normal state, increasing the barrier thickness (and thus  $R_j$ ) will decrease the tunneling probability, thus weakening the magnitude of NSG. However, this is in contradiction with our results.

We now summarize the feature of NSG in PCO: (1) NSG state is not sensitive to magnetic field in all the samples. (2) NSG can be suppressed easily by increasing temperature. (3) The magnitude of NSG is positively associated with  $R_j$ . (4) The magnitude of NSG in the nonsuperconducting samples are further enhanced compared to the superconducting ones.

The Nernst behavior in  $\text{Pr}_{2-x}\text{Ce}_x\text{CuO}_{4\pm\delta}$  discloses that the buildup temperature of superconducting fluctuations always follows the  $T_c$  dome [32]. No matter for the superconducting fluctuations with the Maki-Thompson type or the Aslamazov-Larkin type above  $T_c$ , magnetic field should play a role in pair breaking or phase decoherence [33], and therefore suppress the superconducting fluctuations. However, the NSG state persists in field up to 16 T, even in the nonsuperconducting sample. Besides, the magnitude of the NSG is almost unchanged at  $T = 15$  K by field up to 12 T in PCO [see Fig. 2(d)]. Moreover, we observe enhanced magnitude of NSG in the nonsuperconducting sample. Thus, the superconducting fluctuations should not be the key reason for the NSG.

Several other explanations for the NSG observed in PCO can be also excluded. Coulomb blockade only happens when the thermal fluctuations and quantum fluctuations are low enough [19]. Hopping-dominated conductance between the clusters of disordered-metal-grain-induced ZBA requires samples in deep insulating regime [20]. ZBA in PCO is also unlikely induced by Kondo scattering, due to the pretty small magnetic moment of Pr. The Giaever-Zeller two-step tunneling process is sensitive to magnetic field [34], and should also be ruled out.

Based on our results, we argue that the NSG should stem from disorder-induced electron-electron interactions. Considering the interaction effects in disordered 2D Fermi systems, Altshuler *et al.* obtained a logarithmic-correction density of states. In tunneling experiments, the normalized corrections to the density of states are given by [18,35]

$$\frac{\delta N(\varepsilon)}{N_1} = \frac{1}{4\pi\varepsilon_F\tau} \ln(2\kappa\Delta) \ln(|\varepsilon|\tau), \quad (1)$$

where  $\delta N(\varepsilon)$  is the correction to the density of states,  $N_1$  is unperturbed density of states,  $\varepsilon_F$  is the Fermi energy,  $\tau$  is the relaxation time,  $\Delta$  is the tunneling barrier thickness, and  $\kappa$  is the inverse screening length in 2D. Both  $\tau$  and  $\kappa$  can be used to describe the degree of disorder. Enhancing the degree of disorder will increase the corrections to the density of states. The enhanced  $\Delta$  also leads to a larger  $\delta N$ . The AAL theory was confirmed by a number of tunneling experiments in various disordered metallic films, e.g., Be [36], Ag [37], and In [38] (see Supplemental Material for the scope of the AAL theory [39]). We fit the normalized  $dI/dV$  of various samples with the AAL theory by two parameters, i.e.,  $g = \frac{1}{4\pi\varepsilon_F} \ln(2\kappa\Delta)$  and  $t = e\tau$  [see Figs. 4(c) and 4(d)]. All the data can be well fitted from 2 mV to 8 mV. The deviation at lower bias comes from the thermal broadening effect [14]. At high bias ( $>8$  mV), the deviation results from other effects such as band edge effects [40], the break-down of WKB approximation [41], inelastic electron tunneling process [42], etc. The RRR dependence of the relaxation time  $\tau$  is plotted in the inset of Fig. 4(d), and the nonsuperconducting sample shows a shorter relaxation time than the superconducting ones, indicating an enhanced disorder effect in the nonsuperconducting sample.

Now, we try to understand the behavior of the NSG state in the framework of AAL theory. A small amount of disorder in materials mainly causes two effects, i.e., weak localization

and electron-electron correlations. The former stems from enhanced back-scattering by quantum interference, which leads to a smaller conductance. Magnetic fields destroy the quantum interference, and thus increase the conductivity [43]. The latter originates from the destruction of long-range Coulomb screening. When the disorder-limited mean free path  $l$  is reduced and comparable to the Fermi wavelength, i.e.,  $k_F l \sim 1$ , the density of states near the Fermi energy is suppressed by the enhanced electron-electron Coulomb interactions [18], which is not sensitive to the magnetic field [35]. The electron-electron interactions induce the localization of electrons as the electronic degrees of freedom freeze. With increasing temperature, the localized electrons can gradually overcome the Coulomb interactions due to the thermal excitations, and the reduced density of states rebuilds. In addition,  $R_j$  has a positive correlation with the thickness of the effective barrier. The larger thickness of barrier leads to stronger corrections to the density of states [35]. As mentioned above, the degree of disorder in nonsuperconducting samples is stronger than that in the superconducting ones, which leads to an enhancement in magnitude of NSG.

In conclusion, we observe the NSG state in Ce-free PCO thin films with tunable  $T_c$ . The NSG exhibits field-independence but temperature-dependence for both superconducting and nonsuperconducting samples. Importantly, there is a positive correlation between the magnitude of NSG and the junction resistance, and the magnitude of NSG is further enhanced in nonsuperconducting samples. All these behaviors are in good agreement with AAL theory, indicating that the NSG in electron-doped cuprates stems from disorder-induced electron-electron correlations.

We thank J. A. André for fruitful discussions. This paper was supported by the National Key Basic Research Program of China (Grants No. 2015CB921000 and No. 2016YFA0300301), the National Natural Science Foundation of China (Grants No. 11674374, No. 11574372, and No. 11474338), the Key Research Program of the Chinese Academy of Sciences, (Grant No. XDPB01), the Key Research Program of Frontier Sciences, CAS (Grant No. QYZDB-SSW-SLH008) and the Strategic Priority Research Program of the CAS (Grants No. XDB07020100, No. XDB07020300, and No. XDB07030200), the Beijing Municipal Science and Technology Project (Grant No. Z161100002116011).

- 
- [1] N. P. Armitage, P. Fournier, and R. L. Greene, *Rev. Mod. Phys.* **82**, 2421 (2010).
- [2] D. J. Scalapino, *Rev. Mod. Phys.* **84**, 1383 (2012).
- [3] B. Keimer, S. A. Kivelson, M. R. Norman, S. Uchida, and J. Zaanen, *Nature* **518**, 179 (2015).
- [4] K. Jin, N. P. Butch, K. Kirshenbaum, J. Paglione, and R. L. Greene, *Nature* **476**, 73 (2011).
- [5] X. Zhang, H. Yu, G. He, W. Hu, J. Yuan, B. Zhu, and K. Jin, *Physica C* **525-526**, 18 (2016).
- [6] H. Ding, T. Yokoya, J. C. Campuzano, T. Takahashi, M. Randeria, M. R. Norman, T. Mochiku, K. Kadowaki, and J. Giapintzakis, *Nature* **382**, 51 (1996).
- [7] C. Renner, B. Revaz, J. Y. Genoud, K. Kadowaki, and O. Fischer, *Phys. Rev. Lett.* **80**, 149 (1998).
- [8] M. R. Norman, D. Pines, and C. Kallin, *Adv. Phys.* **54**, 715 (2005).
- [9] J.-H. Ma, Z.-H. Pan, F. C. Niestemski, M. Neupane, Y.-M. Xu, P. Richard, K. Nakayama, T. Sato, T. Takahashi, H.-Q. Luo, L. Fang, H.-H. Wen, Z. Wang, H. Ding, and V. Madhavan, *Phys. Rev. Lett.* **101**, 207002 (2008).
- [10] T. Kondo, R. Khasanov, T. Takeuchi, J. Schmalian, and A. Kaminski, *Nature* **457**, 296 (2009).
- [11] Y. Onose, Y. Taguchi, K. Ishizaka, and Y. Tokura, *Phys. Rev. Lett.* **87**, 217001 (2001).

- [12] N. P. Armitage, F. Ronning, D. H. Lu, C. Kim, A. Damascelli, K. M. Shen, D. L. Feng, H. Eisaki, Z.-X. Shen, P. K. Mang, N. Kaneko, M. Greven, Y. Onose, Y. Taguchi, and Y. Tokura, *Phys. Rev. Lett.* **88**, 257001 (2002).
- [13] Y. Onose, Y. Taguchi, K. Ishizaka, and Y. Tokura, *Phys. Rev. B* **69**, 024504 (2004).
- [14] A. Biswas, P. Fournier, V. N. Smolyaninova, R. C. Budhani, J. S. Higgins, and R. L. Greene, *Phys. Rev. B* **64**, 104519 (2001).
- [15] L. Alff, Y. Krockenberger, B. Welter, M. Schonecke, R. Gross, D. Manske, and M. Naito, *Nature* **422**, 698 (2003).
- [16] Y. Dagan, M. M. Qazilbash, and R. L. Greene, *Phys. Rev. Lett.* **94**, 187003 (2005).
- [17] L. Shan, Y. L. Wang, Y. Huang, S. L. Li, J. Zhao, P. Dai, and H. H. Wen, *Phys. Rev. B* **78**, 014505 (2008).
- [18] B. L. Altshuler, A. G. Aronov, and P. A. Lee, *Phys. Rev. Lett.* **44**, 1288 (1980).
- [19] J. P. Pekola, L. J. Taskinen, and S. Farhangfar, *Appl. Phys. Lett.* **76**, 3747 (2000).
- [20] N. Ossi, L. Bitton, D. B. Gutman, and A. Frydman, *Phys. Rev. B* **87**, 115137 (2013).
- [21] O. Matsumoto, A. Utsuki, A. Tsukada, H. Yamamoto, T. Manabe, and M. Naito, *Physica C* **468**, 1148 (2008).
- [22] G. Chanda, R. P. S. M. Lobo, E. Schachinger, J. Wosnitza, M. Naito, and A. V. Pronin, *Phys. Rev. B* **90**, 024503 (2014).
- [23] Q. X. Jia, T. M. McCleskey, A. K. Burrell, Y. Lin, G. Collis, H. Wang, D. Q. Li, and S. R. Foltyn, *Nat. Mater.* **3**, 529 (2004).
- [24] Y. Lin, H. Wang, M. E. Hawley, S. R. Foltyn, Q. X. Jia, G. Collis, A. K. Burrell, and T. M. McCleskey, *Appl. Phys. Lett.* **85**, 3426 (2004).
- [25] X. J. Wei *et al.* (unpublished).
- [26] See Supplemental Material at <http://link.aps.org/supplemental/10.1103/PhysRevB.96.104518> for the quality characterization of the samples.
- [27] See Supplemental Material at <http://link.aps.org/supplemental/10.1103/PhysRevB.96.104518> for the point contact experimental details.
- [28] P. G. Radaelli, J. D. Jorgensen, A. J. Schultz, J. L. Peng, and R. L. Greene, *Phys. Rev. B* **49**, 15322 (1994).
- [29] J. S. Higgins, Y. Dagan, M. C. Barr, B. D. Weaver, and R. L. Greene, *Phys. Rev. B* **73**, 104510 (2006).
- [30] G. E. Blonder, M. Tinkham, and T. M. Klapwijk, *Phys. Rev. B* **25**, 4515 (1982).
- [31] Y. Krockenberger, H. Yamamoto, A. Tsukada, M. Mitsuhashi, and M. Naito, *Phys. Rev. B* **85**, 184502 (2012).
- [32] P. Li and R. L. Greene, *Phys. Rev. B* **76**, 174512 (2007).
- [33] A. Larkin and A. Varlamov, *Theory of Fluctuations in Superconductors* (Clarendon Press, Oxford, 2005).
- [34] I. Giaever and H. R. Zeller, *Phys. Rev. Lett.* **20**, 1504 (1968).
- [35] P. A. Lee, *Rev. Mod. Phys.* **57**, 287 (1985).
- [36] V. Y. Butko, J. F. DiTusa, and P. W. Adams, *Phys. Rev. Lett.* **84**, 1543 (2000).
- [37] L. H. Yu and D. Natelson, *Phys. Rev. B* **68**, 113407 (2003).
- [38] S. Yoshizawa, H. Kim, Y. Hasegawa, and T. Uchihashi, *Phys. Rev. B* **92**, 041410(R) (2015).
- [39] See Supplemental Material at <http://link.aps.org/supplemental/10.1103/PhysRevB.96.104518> for the scope of the AAL theory.
- [40] Z. Wang, H. Yang, D. Fang, B. Shen, Q. H. Wang, L. Shan, C. Zhang, P. Dai, and H. H. Wen, *Nat. Phys.* **9**, 42 (2012).
- [41] J. Y. T. Wei, C. C. Tsuei, P. J. M. van Bentum, Q. Xiong, C. W. Chu, and M. K. Wu, *Phys. Rev. B* **57**, 3650 (1998).
- [42] J. R. Kirtley and D. J. Scalapino, *Phys. Rev. Lett.* **65**, 798 (1990).
- [43] S. Hikami, A. I. Larkin, and Y. Nagaoka, *Prog. Theor. Phys.* **63**, 707 (1980).